HHS Public Access

Author manuscript

J Mol Cell Cardiol. Author manuscript; available in PMC 2019 January 01.

Published in final edited form as:

J Mol Cell Cardiol. 2018 January ; 114: 72–82. doi:10.1016/j.yjmcc.2017.11.003.

A carvedilol-responsive microRNA, miR-125b-5p protects the heart from acute myocardial infarction by repressing pro-apoptotic bak1 and klf13 in cardiomyocytes

Ahmed S. Bayoumi[1], **Kyoung-mi Park**[1,§], **Yongchao Wang**[1,¶], **Jian-peng Teoh**[1], **Tatsuya Aonuma**[1], **Yaoliang Tang**[1,2], **Huabo Su**[1,3], **Neal L. Weintraub**[1,2], and **Il-man Kim**[1,4]

[1]Vascular Biology Center, Medical College of Georgia, Augusta University, Augusta, GA, USA

[2]Department of Medicine, Medical College of Georgia, Augusta University, Augusta, GA, USA

[3]Department of Pharmacology and Toxicology, Medical College of Georgia, Augusta University, Augusta, GA, USA

[4]Department of Biochemistry and Molecular Biology, Medical College of Georgia, Augusta University, Augusta, GA, USA

Abstract

Background—Cardiac injury is accompanied by dynamic changes in the expression of microRNAs (miRs), small non-coding RNAs that post-transcriptionally regulate target genes. MiR-125b-5p is downregulated in patients with end-stage dilated and ischemic cardiomyopathy, and has been proposed as a biomarker of heart failure. We previously reported that the β-blocker carvedilol promotes cardioprotection via β-arrestin-biased agonism of β_1-adrenergic receptor while stimulating miR-125b-5p processing in the mouse heart. We hypothesize that β_1-adrenergic receptor/β-arrestin1-responsive miR-125b-5p confers the improvement of cardiac function and structure after acute myocardial infarction.

Methods and Results—Using cultured cardiomyocyte (CM) and *in vivo* approaches, we show that miR-125b-5p is an ischemic stress-responsive protector against CM apoptosis. CMs lacking miR-125b-5p exhibit increased susceptibility to stress-induced apoptosis, while CMs overexpressing miR-125b-5p have increased phospho-AKT pro-survival signaling. Moreover, we demonstrate that loss-of-function of miR-125b-5p in the mouse heart causes abnormalities in cardiac structure and function after acute myocardial infarction. Mechanistically, the improvement

Address for correspondence: Il-man Kim, Ph.D., Vascular Biology Center & Department of Biochemistry and Molecular Biology, Medical College of Georgia, Augusta University, CB-3717, 1459 Laney Walker Blvd, Augusta, GA, 30912, USA, Tel: (706) 721-9414, FAX: (706) 721-9799, ilkim@augusta.edu.

§Present address: Washington University, Saint Louis, MO

¶Present address: University of Kentucky, Lexington, KY

Disclosures

The authors declare no conflict of interest.

of cardiac function and structure elicited by miR-125b-5p is in part attributed to repression of the pro-apoptotic genes *Bak1* and *Klf13* in CMs.

Conclusions—In conclusion, these findings reveal a pivotal role for miR-125b-5p in regulating CM survival during acute myocardial infarction.

Graphical abstract

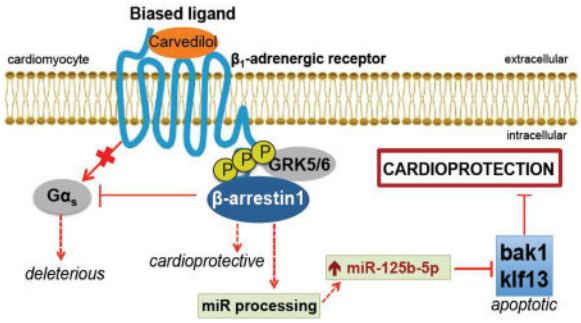

Keywords

β-arrestin; apoptotic genes; biased G protein-coupled receptor signaling; cardioprotection; and microRNAs

Subject Codes

Non-coding RNAs; Cell signaling/signal transduction; Receptor pharmacology; and Heart failure-basic studies

1. Introduction

MicroRNAs (miRNAs or miRs) are increasingly recognized as important regulators of cardiac function and disease [1–3]. We previously showed that the β-blocker carvedilol (Carv) promotes cardioprotection via β-arrestin-biased agonism of β_1-adrenergic receptor (β_1AR) [4, 5]. MiR-125b-5p is one of the five miRs that we found to be activated by Carv [6], and it is downregulated in patients with end-stage dilated cardiomyopathy (DCM) or ischemic cardiomyopathy [7, 8]. Intriguingly, lower levels of miR-125b-5p were also associated with an increased occurrence of acute myocardial infarction (AMI) in humans [9]. In mouse studies, overexpression of miR-125b-5p protected against ischemia/reperfusion (I/R) injury by regulating cardiomyocyte (CM) apoptosis [10], while knockdown of miR-125b-5p suppressed angiotensin II-induced cardiac fibrosis by regulating fibroblast proliferation [11]. Thus, changes in miR-125b-5p expression consequent to cardiac injury and pharmacotherapy may play an important role in cardiac remodeling via several mechanisms. Despite the increasing data from both human and rodent studies, direct evidence demonstrating a role for miR-125b-5p in MI is lacking.

The pro-apoptotic genes *bak1* (mitochondrial protein) and *klf13* (zinc finger transcription factor) have been shown to be regulated by miR-125b-5p in cancer cells [12–16], stem cells [17, 18], neural crest cells and mouse embryos [19]. Notably, *bak1* was significantly

upregulated in mouse hearts during I/R injury and in CMs subjected to simulated I/R [10], as well as in patients with DCM and ischemic heart disease [20]. Moreover, an abnormal copy-number of *klf13* was associated with an increased risk of congenital heart defects in humans [21], and in Xenopus, klf13 has been implicated to play a developmental role in cardiac progenitor cell proliferation and heart morphogenesis [22, 23]. It is unknown, however, whether these two genes are functionally regulated by miR-125b-5p in the post-MI heart.

Here, we show that knockdown of miR-125b-5p alters the pathological responses of the heart to AMI, and that miR-125b-5p acts as a gatekeeper of CM survival by repressing pro-apoptotic *bak1* and *klf13*. Therefore, miR-125b-5p may represent a novel therapeutic target for combating ischemic heart injury.

2. Materials and Methods

2.1. Animal study approval

Eight to 12-week-old C57BL/6 wild-type (WT) mice and 1- to 2-day-old Sprague-Dawley rats were used for this study. Research with animals carried out for this study was performed according to approved protocols and animal welfare regulations of Augusta University's Institutional IACUC Committees. All animal procedures were performed in accordance with NIH guidelines. Neonatal rats were euthanized by decapitation under anesthesia for CM isolation, and mice were euthanized by thoracotomy with 1–4% inhalant isoflurane.

2.2. Mouse model of MI, intramyocardial injection, and post-MI mortality

WT mice (Jackson Laboratory) were subjected to MI as previously published [24]. Briefly, the mice were anesthetized using 1–3% inhalant isoflurane and placed on a heating pad. Animals were intubated and ventilated with medical oxygen using a PhysioSuite MouseVent™ ventilator. The left anterior descending (LAD) coronary artery was visualized under a stereoscope and ligated using an 8-0 prolene suture. Regional ischemia was confirmed by visual inspection under a stereoscope by discoloration of the occluded distal myocardium. Sham-operated animals were subjected to the same procedure without occlusion of the LAD. Immediately after MI or sham surgery, the mice were intramyocardially injected with 0.6mg/kg of miRCURY™ locked nucleic acid-based miR-125b-5p inhibitor (LNA-antimiR-125b-5p) or scrambled anti-miR control (Exiqon) into the ischemic border zone as described previously [25–27]. Briefly, the total volume of single injection was 40 μl and the needle was inserted through the myocardium, without passing into the cardiac lumen. The needle was first advanced in the border peri-infarct zone, covering as much as possible of the infarction perimeter. The antimiRs were then injected while the needle was slowly withdrawn. This technique distributes the antimiRs into a larger area along the perimeter of the infarct zone and a single intracardiac injection of miRs was recently shown to enhance the efficiency in heart tissue [28]. One dose of buprenorphine (0.05mg/kg) was given subcutaneously immediately after the surgery. Responses to toe/skin pinch, heart rate and blood pressure were used for intra- and post-operative monitoring. We also monitored the survival of mice following MI and performed Kaplan-Meier survival analysis.

2.3. Transthoracic echocardiography

Left ventricular performance was assessed by two-dimensional echocardiography using a Visual Sonics Vevo 2100 ultrasound at baseline (pre-surgery) and post-MI (3, 5 and 7 days) as previously described [24]. M-mode tracings were used to measure anterior and posterior wall thicknesses at end diastole and end systole. Left ventricular internal diameter (LVID) was measured in either diastole (LVIDd) or systole (LVIDs). End diastolic volume (EDV) and end systolic volume (ESV) were also measured. A single observer blinded to the experimental groups performed echocardiography and data analysis. Fractional shortening (FS) was calculated according to the following formula: FS (%)=[(LVIDd-LVIDs)/LVIDd] × 100. Ejection fraction (EF) was calculated as: EF (%)=[(EDV- ESV)/EDV] × 100.

2.4. Histology and immunohistochemistry

The hearts were harvested and weighed before undergoing gross anatomical inspection. Morphometric analysis of the heart size was performed as previously published [24]. Histopathological analysis of the cardiac tissues, including fibrosis (Masson's trichrome staining), was performed using standard procedures as previously described [29–32]. For gross histological examination, sections were stained with haematoxylin and eosin (H and E). Myocardial sections were also stained for TUNEL to measure apoptosis using *In Situ* Cell Death Detection Kits (Roche) according to the manufacturer's instructions. The rabbit polyclonal Troponin I antibody (sc-15368, Santa Cruz) was used to visualize CMs.

2.5. Cell culture and transfection

Mouse adult atrial CM HL-1 (obtained from Dr. Claycomb) and rat embryonic ventricular CM H9c2 cell lines were maintained as previously described [24]. Primary neonatal rat ventricular cardiomyocytes (NRVCs) were isolated by dissociation of 1- to 2-day-old Sprague-Dawley rats and maintained as previously published [24]. CMs were transfected with a siRNA control (sc-37007, Santa Cruz), or siRNAs targeting *bak1* (AM16708, Ambion) or *klf13* (4390771, Ambion) with Lipofectamine™ 2000 reagent (Invitrogen) as previously described [4]. To inhibit miR-125b-5p expression in CMs, we transfected mirVana™ miR inhibitors (Life Technologies) specific to miR-125b-5p (MH10148) or a miR inhibitor negative control (4464076) using Lipofectamine™ 2000 reagent (Invitrogen) as described previously [24, 30]. For gain-of-function studies, we transfected mirVana™ miR-125b-5p mimics (Life Technologies, MC10148) or a miR mimic negative control. Transfected cells were incubated overnight in serum-free medium supplemented with 0.1% BSA, 10 mM HEPES (pH 7.4), and 1% penicillin before Carv stimulation. Under serum starvation conditions, CMs were stimulated with Carv (1 μM; Sigma-Aldrich) or dimethyl sulfoxide (DMSO) as a vehicle for 4 hours as described previously [4]. All *in vitro* assays were performed 60–72 hours after transfection when maximum knockdown efficiency was reached.

2.6. *In vitro* simulated ischemia/reperfusion (sI/R) assays

Cells plated on coverslips or 6 well plates were transfected with miR inhibitors, miR mimics or siRNAs as aforementioned, washed, and placed in an ischemia buffer that contained 118mM NaCl, 24mM NaH_2CO_3, 1mM $NaHPO_4$, 2.5mM $CaCl_2$, 1.2mM $MgCl_2$, 20mM

sodium lactate, 16mM KCl and 10mM 2-deoxyglucose (pH 6.2). CMs were then incubated in an anoxic chamber (5% CO_2, 0% O_2) for 1 hour followed by 4 hours of reperfusion-mimicking conditions (by replacing the ischemic buffer with normal cell medium under normoxia conditions) as described [24]. Coverslips or plates were processed for qRT-PCR, immunoblotting and TUNEL staining as mentioned below.

2.7. RNA Isolation and Quantitative Real-Time RT-PCR

Total RNA from CMs and mouse hearts was prepared using Trizol Reagent (Invitrogen) and treated with RNase-free DNase I to remove genomic DNA as described [4, 33, 34]. For detection of mature miR-125b-5p, the TaqMan MicroRNA Reverse Transcription Kit (ThermoFisher Scientific) was used to synthesize cDNA for TaqMan MicroRNA Assays. The following probes (ThermoFisher Scientific), which can detect both rat and mouse miRs, were used to amplify and measure the amount of mature miR by Real-Time RT-PCR: miR-125b-5p, 000449 and U6 snRNA, 001973 for endogenous controls. The following reaction components were used for each probe: 2 μL cDNA, 10 μl 2× TaqMan Universal PCR Master Mix (ThermoFisher Scientific), 1 μl probe, and 7 μl water in a 20 μL total volume.

cDNA for detection of genes was synthesized using ThermoFisher Scientific SuperScript III reverse transcriptase and oligo-dT primers. Expression of genes was detected using Taqman Gene expression assays for mouse or rat (*Anp*, Mm00435329_m1; *Col3a1*, Mm01254476_m1; *Bax*, Mm00432051_m1; *Tnf-α*, Mm00443258_m1; *p53*, Mm00495793_m1; *Bak1*, Mm00432045_m1 or Rn00587491_m1; *Klf13*, Mm00727486_s1 or Rn01477773_m1 and *Hprt1*, Mm00446969_m1 or Rn01527840_m1 for endogenous controls). The following reaction components were used for each probe: 2 μL cDNA, 10 μl 2× TaqMan Universal PCR Master Mix (ThermoFisher Scientific), 1 μl probe, and 7 μl water in a 20 μL total volume.

Real time PCR reactions were amplified and analyzed in triplicate using an ABI Sequence Detection System as described previously [34]. PCR reaction conditions were as follows: Step 1: 50°C for 2 minutes, Step 2: 95°C for 10 minutes, Step 3: 40 cycles of 95°C for 15 seconds followed by 60°C for 1 minute. Expression relative to endogenous controls was calculated using $2^{-\Delta\Delta Ct}$ and levels were normalized to control. We performed at least four independent experiments in triplicate using different batches of RNAs each time.

2.8. Immunoblotting and detection

Cells were washed once with PBS, solubilized in 1 ml of lysis buffer (5 mM HEPES, 250 mM NaCl, 10% glycerol, 0.5% Nonidet P-40, 2 mM EDTA, and protease inhibitors) as previously described [4]. Lysate samples were resolved by SDS-PAGE and transferred to PVDF (Bio-Rad) for immunoblotting. Bak1 (sc-832, Santa Cruz), Klf13 (WH0051621M1, Sigma-Aldrich), β-actin (A2228, Sigma-Aldrich), p-AKT (4060, Cell Signaling) and t-AKT (9272, Cell Signaling) antibodies were purchased and used at dilutions of 1:1,000 each. Detection was carried out using ECL (Amersham Biosciences).

2.9. Cardiomyocyte apoptosis by TUNEL staining

DNA fragmentation was detected *in situ* using TUNEL [24]. In brief, CMs were incubated with proteinase K, and DNA fragments were labeled with fluorescein-conjugated dUTP using terminal deoxynucleotidyl transferase (Roche Diagnostics). The total number of nuclei was determined by manual counting of DAPI-stained nuclei in 6 random fields per coverslip (original magnification, ×200). Digital photographs of fluorescence were acquired with a Zeiss microscope (ApoTome.2; Carl Zeiss) and processed with Adobe Photoshop CS5.1.

2.10. *In silico* miR-125b-5p target prediction analysis

We used several prediction algorithms based on evolutionary conservation of target sites across species including miRDB [35], PicTar [36] and Targetscan [37]. Each of these algorithms predicts hundreds of possible targets for miR-125b-5p, and we focused on putative anti-proliferative or pro-apoptotic targets that were predicted by all of these programs.

2.11. Statistical analysis

Data are expressed as mean ± SEM from at least four independent experiments with different biological samples per group. Statistical significance was determined using one-way ANOVA with Bonferroni correction for multiple comparisons or Student unpaired t-tests (GraphPad Prism version 5). A P value <0.05 was considered statistically significant.

3. Results

3.1. In vivo knockdown of miR-125b-5p results in enhanced post-AMI mortality and left ventricular dysfunction

To investigate the role of miR-125b-5p in experimental MI, we intramyocardially injected LNA™-antimiR-125b-5p into WT mice immediately after LAD occlusion or sham surgery. First, we demonstrated efficacy of the antimiR-125b-5p by showing that the level of miR-125b-5p was reduced, for instance, by ~75% after 7 days compared with anti-miR controls in both the sham and MI groups (Figure 1A and data not shown). We further showed that the hearts of antimiR-125b-5p-injected mice at baseline were functionally normal (Supplementary Table 1–4 and Figure 1C–E), suggesting that miR-125b-5p does not affect cardiac function and structure in the absence of a pathological insult. This conclusion is in line with previous reports in mice with miR-125b-5p knockdown or overexpression at baseline [10, 11].

Despite the normal phenotype at baseline, the mice with knockdown of miR-125b-5p responded differently to ischemic cardiac injury, exhibiting a significant increase in mortality as compared with control mice following ligation of the LAD. The detrimental effect of miR-125b-5p knockdown on survival became obvious 4 days following MI (Figure 1B). Because miR-125b-5p is involved in regulation of the innate immunity [38], which may contribute to ventricular rupture after MI [39], we performed necropsy to detect evidence of hemopericardium. Indeed, knockdown of miR-125b-5p was associated with increased susceptibility to cardiac rupture as compared with anti-miR control (antimiR-125b-5p, 45% compared to anti-miR control, 11%, P<0.01). Moreover, mice with knockdown of

miR-125b-5p developed pronounced left ventricular dysfunction (as evidenced by significantly decreased EF and FS as well as increased LVIDs), and increased ratio of heart weight/body weight at 3 days (Figure 1C–F and Supplementary Table 2), 5 days (Supplementary Table 3) and 7 days (Figure 1C–F and Supplementary Table 4) after MI, when compared to the anti-miR control group.

We also found that anti-miR-125b-5p-injected hearts exhibited more loss of normal architecture and cellular integrity at 3 and 7 days after MI as compared to anti-miR control hearts (Figure 2A), which is consistent with our biochemical data showing that anti-miR-125b-5p-injected hearts had increased mRNA levels of fetal *ANP* and pro-inflammatory *TNF* compared to anti-miR controls (Figure 2B). To further assess the consequence of miR-125b-5p knockdown following MI, we examined fibrosis. Masson's trichrome staining of hearts at 3 and 7 days post-MI revealed small areas of fibrosis in anti-miR control hearts, while the hearts with loss-of-function of miR-125b-5p contained larger fibrotic regions (Figure 2C–D). Anti-miR-125b-5p-injected MI hearts also exhibited increased mRNA levels of fibrotic *Col3a1* compared to anti-miR controls (Figure 2D).

We next demonstrated that anti-miR-125b-5p-injected hearts had higher numbers of TUNEL-positive cells in the heart sections of peri-ischemic border area after 3 and 7 days of MI as compared to anti-miR control MI hearts (Figure 3A). This is consistent with our biochemical data showing that anti-miR-125b-5p-injected hearts had increased mRNA levels of pro-apoptotic *Bax* compared to anti-miR controls (Figure 3B). Because we reported that miR-125b-5p is activated by β_1AR (expressed only in CMs in the heart) [6], and because programmed CM death has been suggested to underlie progressive ventricular remodeling and ischemic cardiac failure [40–43], we next determined whether CMs undergo apoptosis in the mice with loss-of-function of miR-125b-5p. Co-staining for TUNEL and the CM marker troponin I (TnI) demonstrated that knockdown of miR-125b-5p resulted in higher numbers of TUNEL-positive CMs 7 days after MI compared with controls (Figure 3C). Collectively, these results suggest that loss-of-function of miR-125b-5p resulted in diverse pathological abnormalities post-MI, leading to cardiac structural/functional remodeling.

3.2. MiR-125b-5p regulates pro-apoptotic bak1 and klf13

In order to identify candidate miR-125b-5p target genes that regulate cardiac pathology, we used several prediction algorithms including miRDB [35], PicTar [36] and Targetscan [37]. *In silico* ingenuity pathway analysis [44] showed that one of the key associated network functions of the predicted targets of miR-125b-5p is anti-proliferation, cell cycle arrest or apoptosis. Accordingly, we focused on apoptosis-related genes (*bak1, klf13 and p53*) as potential targets of miR-125b-5p.

To identify the functional targets of miR-125b-5p in CMs, we first performed loss- and gain-of-function studies by transfecting anti-miRs and miR mimics to NRVCs, respectively. We were able to achieve downregulation of miR-125b-5p (to over 95% of anti-miR controls) or overexpression of miR-125b-5p (~48-fold of miR mimic controls) (Figure 4A–B). Two of the predicted targets (*bak1* and *klf13*), but not *p53*, were upregulated with miR-125b-5p inhibition and downregulated with miR-125b-5p overexpression (Figure 4C). The mRNA results were confirmed by immunoblotting analysis that demonstrated concordant alterations

in protein levels of bak1 or klf13 after transfection of either miR mimics or anti-miRs for miR-125b-5p, respectively (Figure 4D–E).

These CM results were confirmed *in vivo* by QRT-PCR analyses demonstrating increased levels of *bak1* and *klf13* in anti-miR-125b-5p-injected mouse hearts at both baseline and at 7 days post-MI compared to control (Figure 4F). Importantly, we observed the downregulation of miR-125b-5p in the hearts of WT mice subjected to MI (Figure 4G), which is consistent with several studies in patients with end-stage dilated or ischemic cardiomyopathy [7, 8] as well as AMI [9]. Finally, further mRNA analysis showed that cardiac expression of *bak1* and *klf13* was upregulated following MI as compared with sham control (Figure 4F). These data are consistent with previous studies showing (i) upregulation of cardiac *bak1* in mice following I/R injury and in CMs subjected to simulated I/R [10], as well as in patients with ischemic heart disease [20], and (ii) the upregulation of *klf13* in patients with congenital heart defects [21].

3.3. Carvedilol regulates the miR-125b-5p/bak1 or klf13 pair in cardiomyocytes

We previously showed that Carv upregulates miR-125b-5p in HEK293 cells stably expressing wild-type β_1AR, and in mouse hearts, via stimulating β_1AR, G protein-coupled receptor kinase (GRK) 5/6 and β-arrestin1 [6]. We evaluated the expression of this miR in Carv-treated HL-1 and H9c2 cells as well as NRVCs. Carv modestly upregulated the basal expression of miR-125b-5p and more strongly upregulated its expression following sI/R conditions in HL-1 cells (Figure 5A–B). In H9c2 cells (Figure 5C–D) and NRVCs (Figure 5E–F), Carv only upregulated the expression of miR-125b-5p following sI/R. These data indicate that Carv consistently upregulates miR-125b-5p in injured CMs, and that sI/R predisposes CMs to be more responsive to Carv compared to basal conditions as supported by a previous report that sI/R decreased miR-125b-5p in CMs [10].

Our NRVC data also indicated that Carv decreased the expression of *bak1* and *klf13* following sI/R (Figure 5G–H), concordant with upregulation of miR-125b-5p. Together with the previous studies showing an inverse correlation between miR-125b-5p and bak1 or klf13 in cardiac and CM injury [7–10, 20, 21], our results strongly indicate that *bak1* and *klf13* are functional CM targets of miR-125b-5p. This idea is further supported by previous reports implicating bak1 in cardiac and CM apoptosis [45, 46], and klf13 as a negative regulator of antiapoptotic BCL-X(L) in hematopoietic stem cells, splenocytes, thymocytes, and cancer cells [18, 47, 48].

3.4. MiR-125b-5p functions as a protective miR by repressing pro-apoptotic bak1 and klf13 in CMs

Because our data suggest that pro-apoptotic bak1 and klf13 are regulated by Carv in part via miR-125b-5p, we further hypothesized that miR-125b-5p may function as a pro-survival miR. To determine the importance of miR-125b-5p for CM survival under anoxic conditions, we used *in vitro* models of I/R to show that miR-125b-5p protects CMs from cell death. Loss-offunction of miR-125b-5p in NRVCs increased CM apoptosis (Figure 6A–C). We next tested whether miR-125b-5p activates survival signaling in adult CMs. We observed

that miR-125b-5p overexpression increases p-AKT levels under both basal and simulated I/R conditions (Figure 6D), suggesting that miR-125b-5p acts as a pro-survival miR in CMs.

We next determined if the two targets of miR-125b-5p regulate CM apoptosis. Loss-of-function approaches demonstrated that knockdown of *bak1* or *klf13* decreased NRVC apoptosis in response to sI/R (Figure 7A–E). Finally, to establish a functional linkage between miR-125b-5p, bak1/klf13 expression, and CM apoptosis, we applied a siRNA/antimiR-based rescue strategy to validate the functional relevance of these targets. Consistent with our earlier observations (Figure 6A–C), antimiR-125b-5p alone increased CM apoptosis, while the siRNA against either *bak1* or *klf13* efficiently prevented the pro-apoptotic effects of antimiR-125b-5p (Figure 7). Taken together, our CM data support the *in vivo* evidence that miR-125b-5p exerts protective effects in part through functional repression of pro-apoptotic bak1 and klf13.

4. Discussion

Here, we identify miR-125b-5p as an ischemic stress-responsive protector against CM apoptosis both *in vivo* and *in vitro*. Knockdown of miR-125b-5p renders mice more sensitive to ischemic injury, as evidenced by increased cardiac apoptosis and fibrosis as well as impairment of ventricular function following AMI. Mechanistically, we determined that miR-125b-5p targets pro-apoptotic bak1 and klf13 to elicit its protective effects. CMs deficient in miR-125b-5p exhibit increased sensitivity to sI/R-induced apoptosis, while CMs overexpressing miR-125b-5p have increased pro-survival signaling.

We previously showed that miR-125b-5p is a Carv-responsive miR and is post-transcriptionally activated by β-arrestin1-mediated β_1AR cardioprotective signaling pathways (Figure 8A–C). Together with the results presented here (Figure 8D), we postulate that β-arrestin1-biased β_1AR regulatory mechanism of miR processing in CMs (the only cell type in which β_1ARs are expressed in the heart) may result in beneficial adaptive remodeling following cardiac injury. This hypothesis is further supported by the observation that four Carv/β_1AR/β-arrestin1-responsive miRs (miR-125b-5p, miR-150, miR-199a-3p and miR-214) that we identified [6] are cardioprotective *in vivo* after ischemic injury [10, 24, 49, 50]. Interestingly, two other studies linking Carv to upregulation of cardioprotective miRs have been also reported in rats [51, 52]. Basal expression of the cardioprotective miR-133 [53, 54] in myocardial tissue was significantly upregulated by Carv pretreatment, and upregulation of miR-133 mediated the antiapoptotic action of Carv in isolated CMs [51]. The upregulation of miR-29b, another cardioprotective miR [55], was also shown to contribute to the effects of Carv to attenuate post-MI fibrosis [52]. Collectively, these studies support the concept that the cardioprotective actions of Carv are associated with increased levels of cardioprotective miRs. Notably, miR-125b-5p (miR-125b) is co-transcribed with miR-125b*, which gives rise to two mature forms (a guide -5p strand and a star or passenger -3p strand, respectively) with different seed (targeting) sequences. Although our previous global miR profiling analysis in mouse hearts showed that only miR-125b-5p is post-transcriptionally upregulated by Carv/β_1AR/β-arrestin1-mediated cardioprotective signaling pathways [6], a previous study also demonstrated that miR-125b* contributes to cardioprotection in rats by ischemic pre- and post-conditioning and that overexpression of

the protectomiR confers cytoprotection in NRVCs subjected to sI/R [56]. These studies suggest that the miR-125b family members are regulated by different upstream mechanisms despite their similar association with cardioprotection. Although it would be interesting to investigate the exact role of each miR-125b family member in cardioprotection and the underlying mechanisms, these studies are outside of the scope of the current study to report a novel protective mechanism after AMI by one of Carv-responsive miRs that we identified [6]. Future studies are needed to fully elucidate the possible overlapping/compensatory effects of Carv-responsive miRs and the miR-125b family as well as their underlying mechanisms of action.

Bak1 has been shown to be regulated by miR-125b-5p in cancer cells [12–17], neural crest cells and mouse embryos [19], and CMs and myocardium [10]. *Bak1* was recently identified as a direct target of miR-125b-5p [12, 19]. In addition to reporting that *bak1* is a functional CM target of miR-125b-5p, we demonstrate the novel finding that *klf13* is regulated by miR-125b-5p in CMs, consistent with a report in hematopoietic stem cells [18]. Klf13 has been reported to mediate apoptotic signaling in multiple cell types [18, 47, 48]. In the heart, bak1 was reported to induce CM apoptosis [45] and myocardial I/R-mediated apoptosis [46]. Bak1 expression was also reported to be upregulated in sI/R-induced CMs and I/R-induced mouse hearts [10] as well as in patients' hearts with end stage HF [20]. Gain-of-function variants of *klf13* were associated with increased risk of congenital heart defects in patients [21], and genetic studies in Xenopus showed that klf13 regulates embryonic CM proliferation and heart morphogenesis [22, 23]. Our findings further support that inhibition of *bak1* and *klf13* could be therapeutically beneficial for cardiac disease. Given our data that these two pro-apoptotic genes are functional targets of miR-125b-5p in CMs as well as the previous studies showing an inverse correlation between miR-125b-5p and bak1 or klf13 in cardiac and CM injury [7–10, 20, 21], boosting levels of miR-125b-5p could be therapeutically beneficial to reduce the expression of *bak1* and *klf13* in patients suffering from MI.

Consistent with our findings, two previous studies in a mouse model of either I/R or cecal ligation and puncture (CLP)-induced sepsis reported that overexpression of miR-125b-5p protects the heart from I/R injury or CLP-induced sepsis by inhibiting p53-mediated apoptotic signaling and TRAF6-mediated NF-kB activation [10, 57]. Interestingly, another recent report using loss-of-function approaches showed that miR-125b-5p is maladaptive in angiotensin IIinduced cardiac fibrosis by inhibiting p53 and apelin, subsequently activating cardiac fibroblasts [11]. These contradictory findings likely reflect miR-125b-5p's complex functions depending on the specific cardiac injury model and cell type, as was reported with another Carv/β_1AR/β-arrestin1-regulatable miR, miR-214 [49, 58–60]. Moreover, these previous reports on miR-125b-5p suggest a possible role for miR-125b-5p in post-MI inflammation and cardiac fibroblast activation (i.e. extra-CM effects of miR-125b-5p), which may contribute to the abnormal cardiac remodeling seen in our current study.

Limitations of the study

As recommended by the European Society of Cardiology Working Group on Cellular Biology of the Heart [61, 62], the measurement of infarct size and area at risk may be

required to directly assess acute cardioprotection elicited by miR-125b-5p because it cannot be excluded that the improvement in post-MI cardiac function mediated by miR-125b-5p might be due to other mechanisms, which are not related to acute cardioprotection.

Our previous global profiling analysis identified unique mouse miR signatures regulated by Carv-induced β-arrestin1-biased agonism of β_1AR [6], which may be linked to its mechanism for beneficial adaptive remodeling following cardiac injury. In later studies, we indeed demonstrated that three of Carv-responsive miRs act as protective miRs [24, 63]. We also show in the current study that another Carv-responsive miR, miR-125b-5p confers the improvement of cardiac function and structure after AMI. However, as extensively reviewed in [61, 64, 65], further understanding and more comprehensive analysis of the cardioprotective miR expression profile by using larger scale and unbiased approaches in normal, protected, and comorbid conditions might be warranted to more successfully search novel therapeutic targets because the pathophysiology of ischemic heart disease and cardioprotection is extremely complex.

Conclusions

Our results suggest that miR-125b-5p protects the heart against AMI by blunting CM death in response to injury in part through its repression of bak1 and klf13 (Figure 8D). Although additional mechanistic studies concentrating on miR-125b-5p in different injury models and in other cardiac cell types are needed, our data nevertheless suggest that boosting miR-125b-5p levels to attenuate CM death may provide therapeutic benefits given that downregulation of miR-125b-5p is associated with ischemic cardiomyopathy [7, 8] and AMI [9] in humans.

Supplementary Material

Refer to Web version on PubMed Central for supplementary material.

Acknowledgments

We thank Drs. Ruth Caldwell, Zsolt Bagi and Zheng Dong for sharing their equipment, and Dr. Zuzana Bologna for excellent technical assistance.

Sources of Funding

This work was supported by American Heart Association Predoctoral Fellowship 16PRE30210016 to Jian-peng Teoh, National Institutes of Health R01 HL086555 to Yaoliang Tang, National Institutes of Health R01 HL124248 to Huabo Su, National Institutes of Health R01 HL134354 and AR070029 to Yaoliang Tang and Neal L. Weintraub, National Institutes of Health R01 HL112640 and HL126949 to Neal L. Weintraub, and American Physiological Society Shih-Chun Wang Young Investigator Award, American Heart Association Grant-in-Aid 12GRNT12100048 and Scientist Development Grant 14SDG18970040, and National Institutes of Health R01 HL124251 to Il-man Kim.

Non-Standard Abbreviations and Acronyms

βARs	β-adrenergic receptors
β-blockers	β-adrenergic receptor antagonists
CM	cardiomyocyte

DCM	dilated cardiomyopathy
Carv	carvedilol
GPCR	G protein-coupled receptor
GRK	G protein-coupled receptor kinase
HF	heart failure
I/R	ischemia/reperfusion
KO	knockout
LV	left ventricle
MiRNAs or MiRs	microRNAs
MI	myocardial infarction
NRVCs	neonatal rat ventricular cardiomyocytes
P	phosphorylated
sI/R	simulated ischemia/reperfusion
WT	wild-type

References

1. van Rooij E, Marshall WS, Olson EN. Toward microRNA-based therapeutics for heart disease: the sense in antisense. Circulation research. 2008; 103(9):919–28. [PubMed: 18948630]
2. Catalucci D, Gallo P, Condorelli G. MicroRNAs in cardiovascular biology and heart disease. Circ Cardiovasc Genet. 2009; 2(4):402–8. [PubMed: 20031613]
3. van Rooij E. The art of microRNA research. Circulation research. 2011; 108(2):219–34. [PubMed: 21252150]
4. Kim IM, Tilley DG, Chen J, Salazar NC, Whalen EJ, Violin JD, Rockman HA. Beta-blockers alprenolol and carvedilol stimulate beta-arrestin-mediated EGFR transactivation. Proceedings of the National Academy of Sciences of the United States of America. 2008; 105(38):14555–60. [PubMed: 18787115]
5. Noma T, Lemaire A, Naga Prasad SV, Barki-Harrington L, Tilley DG, Chen J, Le Corvoisier P, Violin JD, Wei H, Lefkowitz RJ, Rockman HA. Beta-arrestin-mediated beta1-adrenergic receptor transactivation of the EGFR confers cardioprotection. J Clin Invest. 2007; 117(9):2445–58. [PubMed: 17786238]
6. Kim IM, Wang Y, Park KM, Tang Y, Teoh JP, Vinson J, Traynham CJ, Pironti G, Mao L, Su H, Johnson JA, Koch WJ, Rockman HA. beta-arrestin1-biased beta1-adrenergic receptor signaling regulates microRNA processing. Circulation research. 2014; 114(5):833–44. [PubMed: 24334028]
7. Voellenkle C, van Rooij J, Cappuzzello C, Greco S, Arcelli D, Di Vito L, Melillo G, Rigolini R, Costa E, Crea F, Capogrossi MC, Napolitano M, Martelli F. MicroRNA signatures in peripheral blood mononuclear cells of chronic heart failure patients. Physiol Genomics. 2010; 42(3):420–6. [PubMed: 20484156]
8. Marques FZ, Vizi D, Khammy O, Mariani JA, Kaye DM. The transcardiac gradient of cardio-microRNAs in the failing heart. Eur J Heart Fail. 2016

9. Huang S, Chen M, Li L, He M, Hu D, Zhang X, Li J, Tanguay RM, Feng J, Cheng L, Zeng H, Dai X, Deng Q, Hu FB, Wu T. Circulating MicroRNAs and the occurrence of acute myocardial infarction in Chinese populations. Circ Cardiovasc Genet. 2014; 7(2):189–98. [PubMed: 24627568]
10. Wang X, Ha T, Zou J, Ren D, Liu L, Zhang X, Kalbfleisch J, Gao X, Williams D, Li C. MicroRNA-125b protects against myocardial ischaemia/reperfusion injury via targeting p53-mediated apoptotic signalling and TRAF6. Cardiovasc Res. 2014; 102(3):385–95. [PubMed: 24576954]
11. Nagpal V, Rai R, Place AT, Murphy SB, Verma SK, Ghosh AK, Vaughan DE. MiR-125b Is Critical for Fibroblast-to-Myofibroblast Transition and Cardiac Fibrosis. Circulation. 2016; 133(3):291–301. [PubMed: 26585673]
12. Li Q, Wu Y, Zhang Y, Sun H, Lu Z, Du K, Fang S, Li W. miR-125b regulates cell progression in chronic myeloid leukemia via targeting BAK1. Am J Transl Res. 2016; 8(2):447–59. [PubMed: 27158338]
13. Zeng QH, Xu L, Liu XD, Liao W, Yan MX. miR-125b promotes proliferation of human acute myeloid leukemia cells by targeting Bak1. Zhonghua Xue Ye Xue Za Zhi. 2013; 34(12):1010–4. [PubMed: 24369155]
14. Kong F, Sun C, Wang Z, Han L, Weng D, Lu Y, Chen G. miR-125b confers resistance of ovarian cancer cells to cisplatin by targeting pro-apoptotic Bcl-2 antagonist killer 1. J Huazhong Univ Sci Technolog Med Sci. 2011; 31(4):543–9. [PubMed: 21823019]
15. Zhou M, Liu Z, Zhao Y, Ding Y, Liu H, Xi Y, Xiong W, Li G, Lu J, Fodstad O, Riker AI, Tan M. MicroRNA-125b confers the resistance of breast cancer cells to paclitaxel through suppression of pro-apoptotic Bcl-2 antagonist killer 1 (Bak1) expression. J Biol Chem. 2010; 285(28):21496–507. [PubMed: 20460378]
16. Shi XB, Xue L, Yang J, Ma AH, Zhao J, Xu M, Tepper CG, Evans CP, Kung HJ, deVere White RW. An androgen-regulated miRNA suppresses Bak1 expression and induces androgen-independent growth of prostate cancer cells. Proceedings of the National Academy of Sciences of the United States of America. 2007; 104(50):19983–8. [PubMed: 18056640]
17. Chen J, Fu X, Wan Y, Wang Z, Jiang D, Shi L. miR-125b inhibitor enhance the chemosensitivity of glioblastoma stem cells to temozolomide by targeting Bak1. Tumour Biol. 2014; 35(7):6293–302. [PubMed: 24643683]
18. Ooi AG, Sahoo D, Adorno M, Wang Y, Weissman IL, Park CY. MicroRNA-125b expands hematopoietic stem cells and enriches for the lymphoid-balanced and lymphoid-biased subsets. Proceedings of the National Academy of Sciences of the United States of America. 2010; 107(50): 21505–10. [PubMed: 21118986]
19. Chen X, Liu J, Feng WK, Wu X, Chen SY. MiR-125b protects against ethanol-induced apoptosis in neural crest cells and mouse embryos by targeting Bak 1 and PUMA. Exp Neurol. 2015; 271:104–11. [PubMed: 26024858]
20. Latif N, Khan MA, Birks E, O'Farrell A, Westbrook J, Dunn MJ, Yacoub MH. Upregulation of the Bcl-2 family of proteins in end stage heart failure. J Am Coll Cardiol. 2000; 35(7):1769–77. [PubMed: 10841223]
21. Derwinska K, Bartnik M, Wisniowiecka-Kowalnik B, Jagla M, Rudzinski A, Pietrzyk JJ, Kawalec W, Ziolkowska L, Kutkowska-Kazmierczak A, Gambin T, Sykulski M, Shaw CA, Gambin A, Mazurczak T, Obersztyn E, Bocian E, Stankiewicz P. Assessment of the role of copy-number variants in 150 patients with congenital heart defects. Med Wieku Rozwoj. 2012; 16(3):175–82. [PubMed: 23378395]
22. Nemer M, Horb ME. The KLF family of transcriptional regulators in cardiomyocyte proliferation and differentiation. Cell Cycle. 2007; 6(2):117–21. [PubMed: 17245133]
23. Lavallee G, Andelfinger G, Nadeau M, Lefebvre C, Nemer G, Horb ME, Nemer M. The Kruppel-like transcription factor KLF13 is a novel regulator of heart development. The EMBO journal. 2006; 25(21):5201–13. [PubMed: 17053787]
24. Tang Y, Wang Y, Park KM, Hu Q, Teoh JP, Broskova Z, Ranganathan P, Jayakumar C, Li J, Su H, Ramesh G, Kim IM. MicroRNA-150 Protects the Mouse Heart from Ischemic Injury by Regulating Cell Death. Cardiovasc Res. 2015

25. Tang YL, Tang Y, Zhang YC, Qian K, Shen L, Phillips MI. Protection from ischemic heart injury by a vigilant heme oxygenase-1 plasmid system. Hypertension. 2004; 43(4):746–51. [PubMed: 14981066]
26. Arnold AS, Tang YL, Qian K, Shen L, Valencia V, Phillips MI, Zhang YC. Specific beta1-adrenergic receptor silencing with small interfering RNA lowers high blood pressure and improves cardiac function in myocardial ischemia. J Hypertens. 2007; 25(1):197–205. [PubMed: 17143192]
27. Chen L, Ashraf M, Wang Y, Zhou M, Zhang J, Qin G, Rubinstein J, Weintraub NL, Tang Y. The role of notch 1 activation in cardiosphere derived cell differentiation. Stem Cells Dev. 2012; 21(12):2122–9. [PubMed: 22239539]
28. Lesizza P, Prosdocimo G, Martinelli V, Sinagra G, Zacchigna S, Giacca M. Single-Dose Intracardiac Injection of Pro-Regenerative MicroRNAs Improves Cardiac Function After Myocardial Infarction. Circ Res. 2017; 120(8):1298–1304. [PubMed: 28077443]
29. Ramakrishna S, Kim IM, Petrovic V, Malin D, Wang IC, Kalin TV, Meliton L, Zhao YY, Ackerson T, Qin Y, Malik AB, Costa RH, Kalinichenko VV. Myocardium defects and ventricular hypoplasia in mice homozygous null for the Forkhead Box M1 transcription factor. Dev Dyn. 2007; 236(4): 1000–13. [PubMed: 17366632]
30. Kim IM, Ackerson T, Ramakrishna S, Tretiakova M, Wang IC, Kalin TV, Major ML, Gusarova GA, Yoder HM, Costa RH, Kalinichenko VV. The Forkhead Box m1 transcription factor stimulates the proliferation of tumor cells during development of lung cancer. Cancer Res. 2006; 66(4):2153–61. [PubMed: 16489016]
31. Chatterjee TK, Basford JE, Knoll E, Tong WS, Blanco V, Blomkalns AL, Rudich S, Lentsch AB, Hui DY, Weintraub NL. HDAC9 knockout mice are protected from adipose tissue dysfunction and systemic metabolic disease during high fat feeding. Diabetes. 2013
32. Blomkalns AL, Gavrila D, Thomas M, Neltner BS, Blanco VM, Benjamin SB, McCormick ML, Stoll LL, Denning GM, Collins SP, Qin Z, Daugherty A, Cassis LA, Thompson RW, Weiss RM, Lindower PD, Pinney SM, Chatterjee T, Weintraub NL. CD14 directs adventitial macrophage precursor recruitment: role in early abdominal aortic aneurysm formation. J Am Heart Assoc. 2013; 2(2):e000065. [PubMed: 23537804]
33. Kim IM, Ramakrishna S, Gusarova GA, Yoder HM, Costa RH, Kalinichenko VV. The forkhead box m1 transcription factor is essential for embryonic development of pulmonary vasculature. J Biol Chem. 2005; 280(23):22278–86. [PubMed: 15817462]
34. Kim IM, Wolf MJ, Rockman HA. Gene deletion screen for cardiomyopathy in adult Drosophila identifies a new notch ligand. Circulation research. 2010; 106(7):1233–43. [PubMed: 20203305]
35. Wang X. miRDB: a microRNA target prediction and functional annotation database with a wiki interface. Rna. 2008; 14(6):1012–7. [PubMed: 18426918]
36. Krek A, Grun D, Poy MN, Wolf R, Rosenberg L, Epstein EJ, MacMenamin P, da Piedade I, Gunsalus KC, Stoffel M, Rajewsky N. Combinatorial microRNA target predictions. Nat Genet. 2005; 37(5):495–500. [PubMed: 15806104]
37. Lewis BP, Shih IH, Jones-Rhoades MW, Bartel DP, Burge CB. Prediction of mammalian microRNA targets. Cell. 2003; 115(7):787–98. [PubMed: 14697198]
38. Zhang XH, Zhang YN, Li HB, Hu CY, Wang N, Cao PP, Liao B, Lu X, Cui YH, Liu Z. Overexpression of miR-125b, a novel regulator of innate immunity, in eosinophilic chronic rhinosinusitis with nasal polyps. Am J Respir Crit Care Med. 2012; 185(2):140–51. [PubMed: 22071331]
39. Yan X, Shichita T, Katsumata Y, Matsuhashi T, Ito H, Ito K, Anzai A, Endo J, Tamura Y, Kimura K, Fujita J, Shinmura K, Shen W, Yoshimura A, Fukuda K, Sano M. Deleterious effect of the IL-23/IL-17A axis and gammadeltaT cells on left ventricular remodeling after myocardial infarction. J Am Heart Assoc. 2012; 1(5):e004408. [PubMed: 23316306]
40. Haudek SB, Taffet GE, Schneider MD, Mann DL. TNF provokes cardiomyocyte apoptosis and cardiac remodeling through activation of multiple cell death pathways. The Journal of clinical investigation. 2007; 117(9):2692–701. [PubMed: 17694177]
41. Fliss H, Gattinger D. Apoptosis in ischemic and reperfused rat myocardium. Circulation research. 1996; 79(5):949–56. [PubMed: 8888687]

42. Shukla PC, Singh KK, Quan A, Al-Omran M, Teoh H, Lovren F, Cao L, Rovira II, Pan Y, Brezden-Masley C, Yanagawa B, Gupta A, Deng CX, Coles JG, Leong-Poi H, Stanford WL, Parker TG, Schneider MD, Finkel T, Verma S. BRCA1 is an essential regulator of heart function and survival following myocardial infarction. Nat Commun. 2011; 2:593. [PubMed: 22186889]
43. Khand A, Gemmel I, Clark AL, Cleland JG. Is the prognosis of heart failure improving? J Am Coll Cardiol. 2000; 36(7):2284–6. [PubMed: 11127474]
44. Werner T. Bioinformatics applications for pathway analysis of microarray data. Curr Opin Biotechnol. 2008; 19(1):50–4. [PubMed: 18207385]
45. Ing DJ, Zang J, Dzau VJ, Webster KA, Bishopric NH. Modulation of cytokine-induced cardiac myocyte apoptosis by nitric oxide, Bak, and Bcl-x. Circ Res. 1999; 84(1):21–33. [PubMed: 9915771]
46. Zhao S, Lin Q, Li H, He Y, Fang X, Chen F, Chen C, Huang Z. Carbon monoxide releasing molecule2 attenuated ischemia/reperfusioninduced apoptosis in cardiomyocytes via a mitochondrial pathway. Mol Med Rep. 2014; 9(2):754–62. [PubMed: 24337106]
47. Zhou M, McPherson L, Feng D, Song A, Dong C, Lyu SC, Zhou L, Shi X, Ahn YT, Wang D, Clayberger C, Krensky AM. Kruppel-like transcription factor 13 regulates T lymphocyte survival in vivo. J Immunol. 2007; 178(9):5496–504. [PubMed: 17442931]
48. Fernandez-Zapico ME, Lomberk GA, Tsuji S, DeMars CJ, Bardsley MR, Lin YH, Almada LL, Han JJ, Mukhopadhyay D, Ordog T, Buttar NS, Urrutia R. A functional family-wide screening of SP/KLF proteins identifies a subset of suppressors of KRAS-mediated cell growth. Biochem J. 2011; 435(2):529–37. [PubMed: 21171965]
49. Aurora AB, Mahmoud AI, Luo X, Johnson BA, van Rooij E, Matsuzaki S, Humphries KM, Hill JA, Bassel-Duby R, Sadek HA, Olson EN. MicroRNA-214 protects the mouse heart from ischemic injury by controlling Ca(2)(+) overload and cell death. The Journal of clinical investigation. 2012; 122(4):1222–32. [PubMed: 22426211]
50. Eulalio A, Mano M, Dal Ferro M, Zentilin L, Sinagra G, Zacchigna S, Giacca M. Functional screening identifies miRNAs inducing cardiac regeneration. Nature. 2012; 492(7429):376–81. [PubMed: 23222520]
51. Xu C, Hu Y, Hou L, Ju J, Li X, Du N, Guan X, Liu Z, Zhang T, Qin W, Shen N, Bilal MU, Lu Y, Zhang Y, Shan H. beta-Blocker carvedilol protects cardiomyocytes against oxidative stress-induced apoptosis by up-regulating miR-133 expression. J Mol Cell Cardiol. 2014; 75:111–21. [PubMed: 25066695]
52. Zhu JN, Chen R, Fu YH, Lin QX, Huang S, Guo LL, Zhang MZ, Deng CY, Zou X, Zhong SL, Yang M, Zhuang J, Yu XY, Shan ZX. Smad3 inactivation and MiR-29b upregulation mediate the effect of carvedilol on attenuating the acute myocardium infarction-induced myocardial fibrosis in rat. PLoS ONE. 2013; 8(9):e75557. [PubMed: 24086569]
53. Matkovich SJ, Wang W, Tu Y, Eschenbacher WH, Dorn LE, Condorelli G, Diwan A, Nerbonne JM, Dorn GW 2nd. MicroRNA-133a protects against myocardial fibrosis and modulates electrical repolarization without affecting hypertrophy in pressure-overloaded adult hearts. Circulation research. 2010; 106(1):166–75. [PubMed: 19893015]
54. Castaldi A, Zaglia T, Di Mauro V, Carullo P, Viggiani G, Borile G, Di Stefano B, Schiattarella GG, Gualazzi MG, Elia L, Stirparo GG, Colorito ML, Pironti G, Kunderfranco P, Esposito G, Bang ML, Mongillo M, Condorelli G, Catalucci D. MicroRNA-133 modulates the beta1-adrenergic receptor transduction cascade. Circulation research. 2014; 115(2):273–83. [PubMed: 24807785]
55. Zhang Y, Huang XR, Wei LH, Chung AC, Yu CM, Lan HY. miR-29b as a therapeutic agent for angiotensin II-induced cardiac fibrosis by targeting TGF-beta/Smad3 signaling. Mol Ther. 2014; 22(5):974–85. [PubMed: 24569834]
56. Varga ZV, Zvara A, Farago N, Kocsis GF, Pipicz M, Gaspar R, Bencsik P, Gorbe A, Csonka C, Puskas LG, Thum T, Csont T, Ferdinandy P. MicroRNAs associated with ischemia-reperfusion injury and cardioprotection by ischemic pre- and postconditioning: protectomiRs. Am J Physiol Heart Circ Physiol. 2014; 307(2):H216–27. [PubMed: 24858849]
57. Ma H, Wang X, Ha T, Gao M, Liu L, Wang R, Yu K, Kalbfleisch JH, Kao RL, Williams DL, Li C. MicroRNA-125b Prevents Cardiac Dysfunction in Polymicrobial Sepsis by Targeting TRAF6-Mediated Nuclear Factor kappaB Activation and p53-Mediated Apoptotic Signaling. J Infect Dis. 2016; 214(11):1773–1783. [PubMed: 27683819]

58. Yang X, Qin Y, Shao S, Yu Y, Zhang C, Dong H, Lv G, Dong S. MicroRNA-214 Inhibits Left Ventricular Remodeling in an Acute Myocardial Infarction Rat Model by Suppressing Cellular Apoptosis via the Phosphatase and Tensin Homolog (PTEN). Int Heart J. 2016; 57(2):247–50. [PubMed: 26973267]

59. Sun M, Yu H, Zhang Y, Li Z, Gao W. MicroRNA-214 Mediates Isoproterenol-induced Proliferation and Collagen Synthesis in Cardiac Fibroblasts. Sci Rep. 2015; 5:18351. [PubMed: 26692091]

60. Yang T, Gu H, Chen X, Fu S, Wang C, Xu H, Feng Q, Ni Y. Cardiac hypertrophy and dysfunction induced by overexpression of miR-214 in vivo. J Surg Res. 2014; 192(2):317–25. [PubMed: 25085702]

61. Hausenloy DJ, Garcia-Dorado D, Botker HE, Davidson SM, Downey J, Engel FB, Jennings R, Lecour S, Leor J, Madonna R, Ovize M, Perrino C, Prunier F, Schulz R, Sluijter JPG, Van Laake LW, Vinten-Johansen J, Yellon DM, Ytrehus K, Heusch G, Ferdinandy P. Novel targets and future strategies for acute cardioprotection: Position Paper of the European Society of Cardiology Working Group on Cellular Biology of the Heart. Cardiovasc Res. 2017; 113(6):564–585. [PubMed: 28453734]

62. Lecour S, Botker HE, Condorelli G, Davidson SM, Garcia-Dorado D, Engel FB, Ferdinandy P, Heusch G, Madonna R, Ovize M, Ruiz-Meana M, Schulz R, Sluijter JP, Van Laake LW, Yellon DM, Hausenloy DJ. ESC working group cellular biology of the heart: position paper: improving the preclinical assessment of novel cardioprotective therapies. Cardiovasc Res. 2014; 104(3):399–411. [PubMed: 25344369]

63. Park KM, Teoh JP, Wang Y, Broskova Z, Bayoumi AS, Tang Y, Su H, Weintraub NL, Kim IM. Carvedilol-responsive microRNAs, miR-199a-3p and -214 protect cardiomyocytes from simulated ischemia-reperfusion injury. Am J Physiol Heart Circ Physiol. 2016; 311(2):H371–83. [PubMed: 27288437]

64. Perrino C, Barabasi AL, Condorelli G, Davidson SM, De Windt L, Dimmeler S, Engel FB, Hausenloy DJ, Hill JA, Van Laake LW, Lecour S, Leor J, Madonna R, Mayr M, Prunier F, Sluijter JPG, Schulz R, Thum T, Ytrehus K, Ferdinandy P. Epigenomic and transcriptomic approaches in the post-genomic era: path to novel targets for diagnosis and therapy of the ischaemic heart? Position Paper of the European Society of Cardiology Working Group on Cellular Biology of the Heart. Cardiovasc Res. 2017; 113(7):725–736. [PubMed: 28460026]

65. Varga ZV, Giricz Z, Bencsik P, Madonna R, Gyongyosi M, Schulz R, Mayr M, Thum T, Puskas LG, Ferdinandy P. Functional Genomics of Cardioprotection by Ischemic Conditioning and the Influence of Comorbid Conditions: Implications in Target Identification. Curr Drug Targets. 2015; 16(8):904–11. [PubMed: 25915487]

Highlights

- MiR-125b-5p protects the heart against myocardial infarction.
- MiR-125b-5p functions as a gatekeeper of cardiomyocyte survival.
- The action of miR-125b-5p is mediated by the repression of *bak1* and *klf13*.

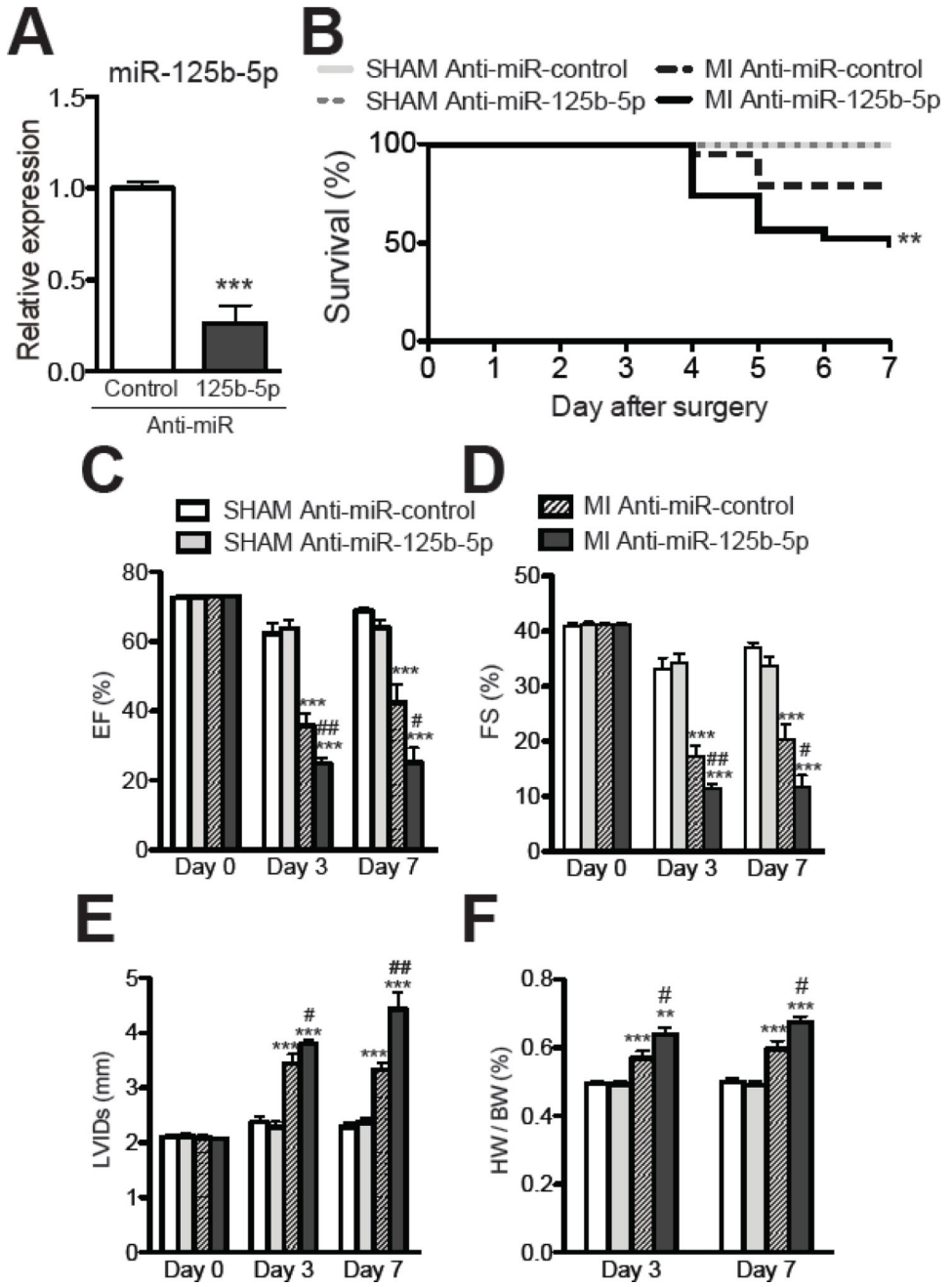

Figure 1. MiR-125b-5p protects the mouse heart against AMI

A, QRT-PCR expression analysis of miR-125b-5p in hearts from WT mice intramyocardially injected with 0.6mg/kg of LNA™ miR-125b-5p inhibitor (antimiR-125bp-5p) or scrambled anti-miR control for 7 days. N=4 per group; data are shown as fold induction of miR-125b-5p expression normalized to U6 snRNA and expressed as mean ± SEM. ***P<0.001 vs. anti-miR control. **B**, Survival curve following MI in mice injected with antimiR-125b-5p and scrambled anti-miR control. N=16–22, **P<0.01 vs. all other groups. **C–E**, Transthoracic echocardiography was performed at 3 and 7 days post-MI by a blinded investigator on age/sex-matched mice. Quantification of left ventricular (LV)

ejection fraction (EF: **C**), fractional shortening (FS: **D**), and LV internal diameter, systole (LVIDs: **E**) is shown. N=7–20; data represent mean ± SEM. ***P<0.001 vs. Sham; $^{\#}P$<0.05 or $^{\#\#}P$<0.01 vs. all other groups. **F,** heart weight/body weight (HW/BW) ratio of WT mice injected with either anti-miR-125b-5p or anti-miR control (N=4–6). Data represent mean ± SEM. **P<0.01 or ***P<0.001 vs. Sham; $^{\#}P$<0.05 vs. all other groups.

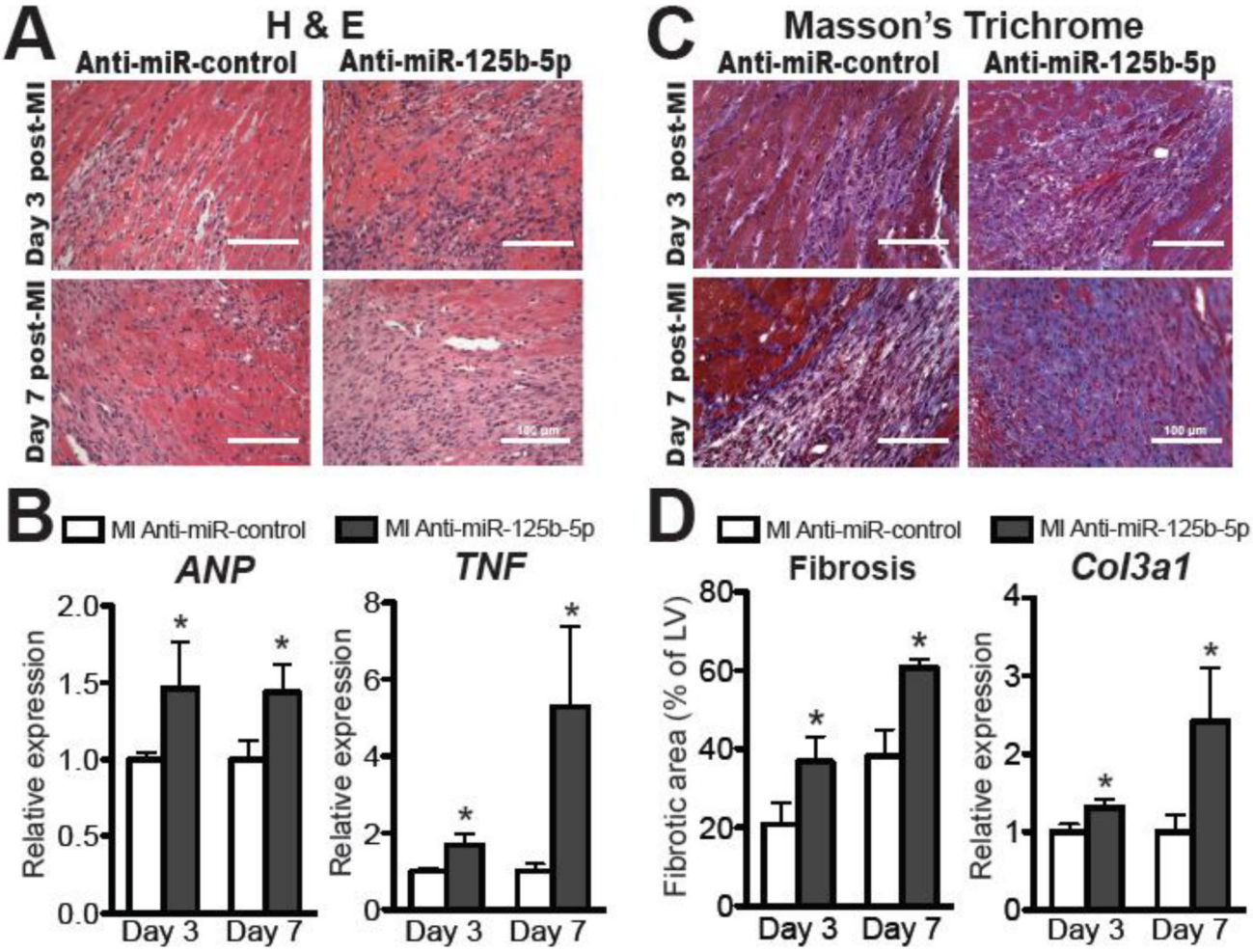

Figure 2. Knockdown of miR-125b-5p induces abnormalities in cardiac structure and expression of genes involved in cardiac stress, inflammation, and fibrosis post-AMI

A, Representative H & E staining of transverse heart sections of peri-ischemic border area at 3 and 7 days post-MI demonstrates more loss of normal architecture and cellular integrity in anti-miR-125b-5p-injected hearts compared to anti-miR controls. **B**, QRT-PCR analysis of gene expression (*ANP*: cardiac stress and *TNF-α*: inflammation) in the post-infarcted hearts from anti-miR-125b-5p-injected mice compared to anti-miR controls at 3 and 7 days post-MI. N=3–5 per group; data are shown as fold induction of gene expression normalized to *Hprt1* and expressed as mean ± SEM. **P*<0.05 vs. MI anti-miR control. **C–D**, Representative Masson's trichrome staining (**C**) and quantification of fibrosis (**D**, left) in transverse heart sections of peri-ischemic border area at 3 and 7 days post-MI. **D**, (Right) QRT-PCR analysis of fibrotic *Col3a1* expression in anti-miR-125b-5p-injected hearts relative to anti-miR controls at post-MI day 3 and 7. N=3–5 per group; data are shown as fold induction of *Col3a1* expression normalized to *Hprt1* and expressed as mean ± SEM. **P*<0.05 vs. MI anti-miR control.

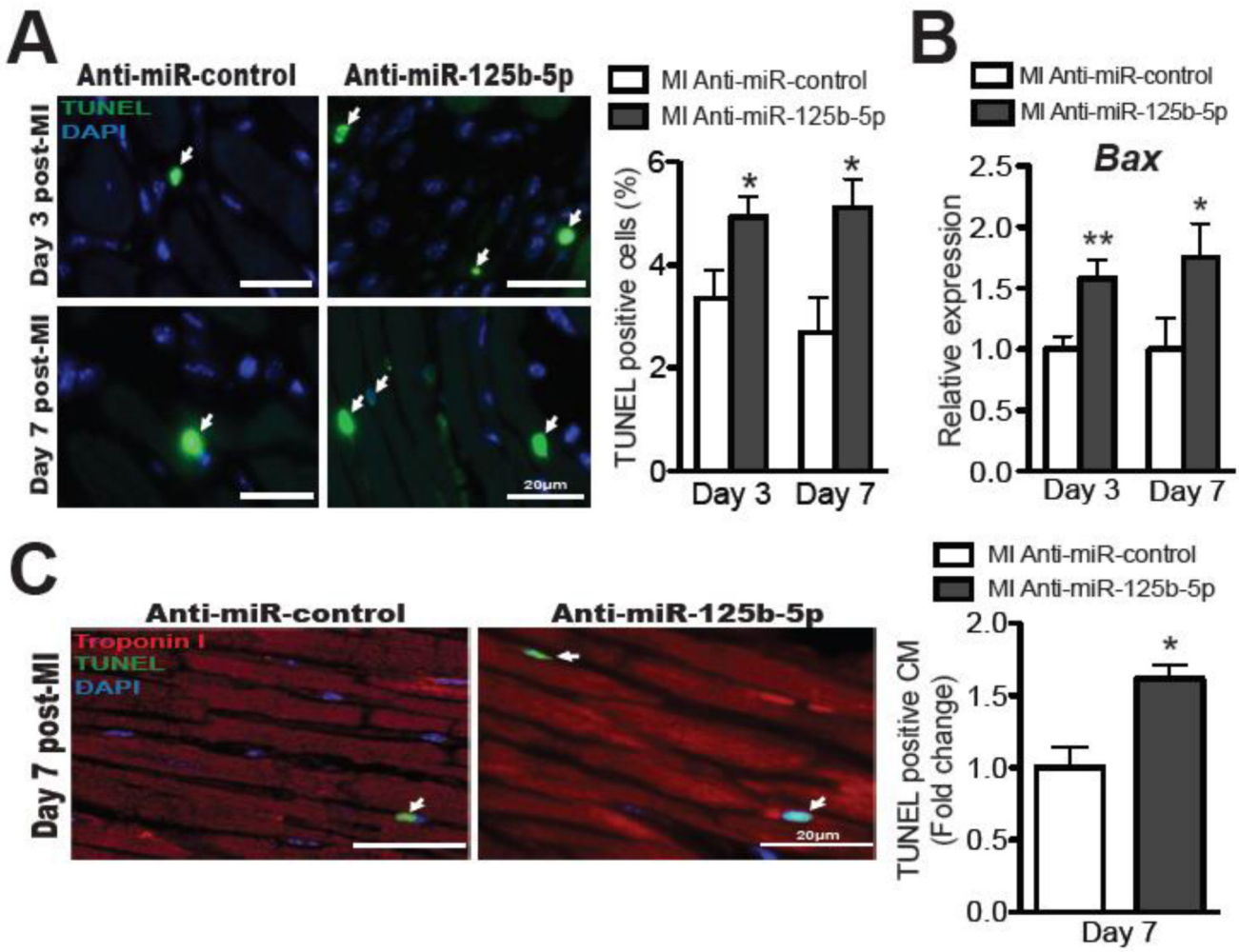

Figure 3. MiR-125b-5p knockdown increases cardiomyocyte apoptosis post-AMI

A, Representative TUNEL staining (left) and quantification (right) of transverse heart sections of peri-ischemic border area at 3 and 7 days post-MI show increased apoptosis in anti-miR-125b-5p-injected hearts compared to anti-miR controls. **B**, QRT-PCR expression analysis of apoptotic *Bax* in anti-miR-125b-5p-injected hearts relative to anti-miR controls at 3 and 7 days post-MI. N=3–7 per group; data are shown as fold induction of gene expression normalized to *Hprt1* and expressed as mean ± SEM. **P*<0.05 or ***P*<0.01 vs. MI anti-miR control. **C**, (Left) Immunohistochemistry for TUNEL (green) and troponin I (red) with DAPI counterstain (blue) of transverse sections of hearts injected with anti-miR-125b-5p and anti-miR controls at day 7 post-MI. (Right) Quantification of apoptotic cardiomyocytes (CMs; TUNEL- and troponin I-positive) in the peri-ischemic border area of transverse heart sections at day 7 post-MI. Representative results are from 9 random 63× fields per sample, N=3–4. Data represent mean ± SEM; **P* < 0.05 vs. MI anti-miR controls.

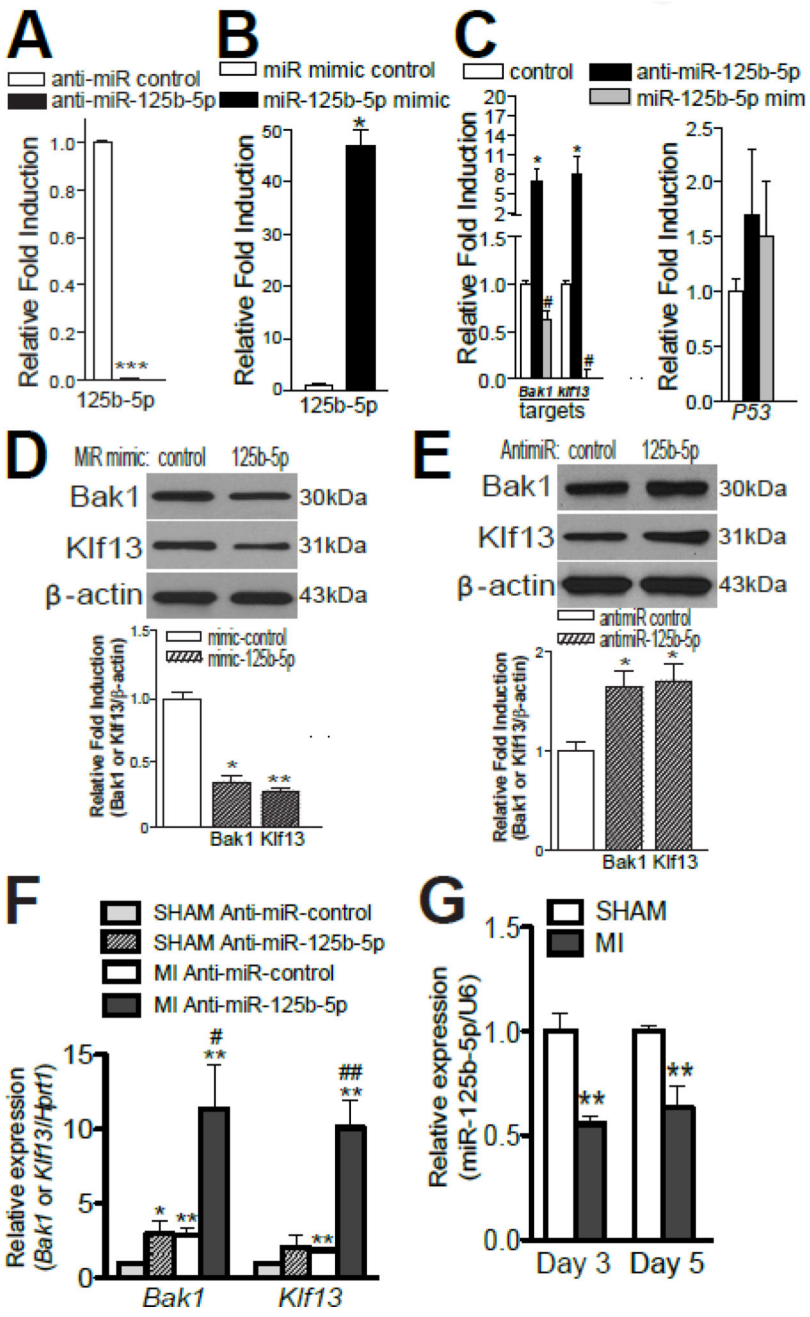

Figure 4. MiR-125b-5p represses pro-apoptotic *bak1* and *klf13*

A–C, RNAs isolated from NRVCs transfected with 100nM *mir*vana miR-125b-5p inhibitor or 15-mer control (**A**) and miR-125b-5p mimic or 15-mer control (**B**) were analyzed by miR-125b-5p-specific RT-PCR and QRT-PCR to access the levels of miR-125b-5p. $^{*}P <$ 0.05 vs. miR mimic control; $^{***}P < 0.001$ vs. anti-miR control. Levels of miR-125b-5p's predicted target mRNAs are shown in **C**. Data were normalized to *Hprt1* and expressed relative to control (anti-miR control or miR mimic control). Results are representative of 4 independent experiments with different biological samples. $^{*}P < 0.05$ or $^{\#}P < 0.05$ vs. control. **D–E**, Gain- or loss-of-function of miR-125b-5p in NRVCs resulted in decreased (**D**)

or increased (**E**) bak1 or klf13 protein levels, respectively. N=4. *$P < 0.05$ or **$P < 0.01$ vs. control. **F,** *Bak1* and *klf13* mRNA levels were measured in lysates of left ventricular tissues from anti-miR-125b-5p-injected mice compared to anti-miR controls at baseline and at 7 days post-MI. N=4–8. *$P < 0.05$ or **$P < 0.01$ vs. sham anti-miR control; $^{\#}P < 0.05$ or $^{\#\#}P < 0.05$ vs. other three groups. **G**, QRT-PCR expression analysis of miR-125b-5p in left ventricular tissues at 3 and 5 days post-MI. **$P < 0.01$ vs. sham.

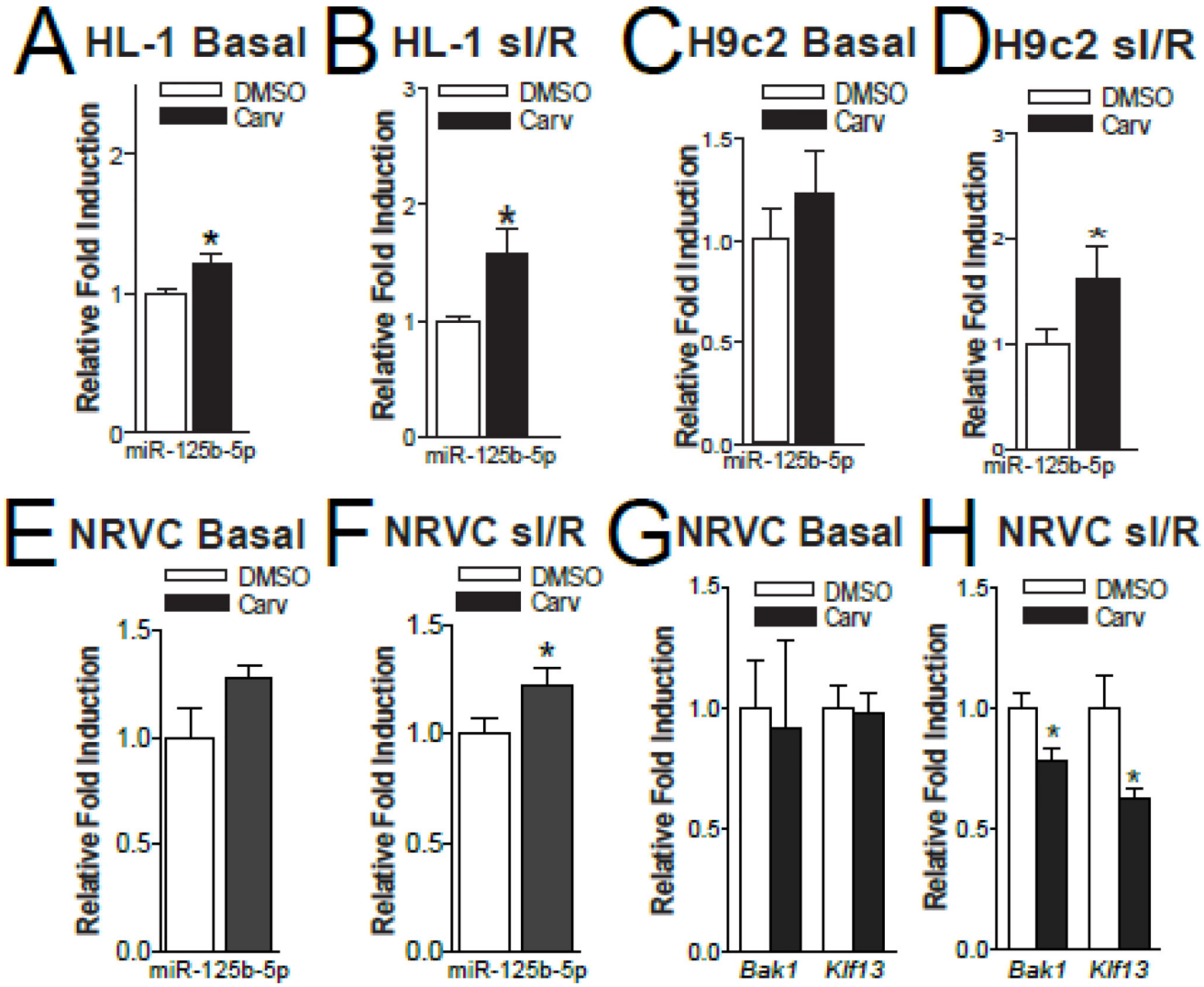

Figure 5. Carvedilol induces the expression of miR-125b-5p in simulated ischemia/reperfusion in both atrial and ventricular CMs, and inhibits the expression of its targets *bak1* or *klf13* in NRVCs

A–B, The expression of mature miR-125b-5p in HL-1 cells treated with either vehicle (DMSO) or 1μM of carvedilol (Carv) for 4 hours and subjected to either normoxia (basal) or simulated ischemia/reperfusion (sI/R). **C–D**, The expression of mature miR-125b-5p in H9c2 cells treated with 1μM of Carv for 4 hours and subjected to either normoxia (basal) or sI/R. N=5 in each group. **P* < 0.05 vs. DMSO. **E–F**, QRT-PCR analysis of miR-125b-5p in NRVCs treated with 1μM Carv for 4 hours and subjected to either normoxia (basal) or sI/R. **G–H**, QRT-PCR analysis of *bak1* and *klf13* in NRVCs treated with 1μM of Carv for 4 hours and subjected to either normoxia (basal) or sI/R. N=6. **P* < 0.05 vs. DMSO.

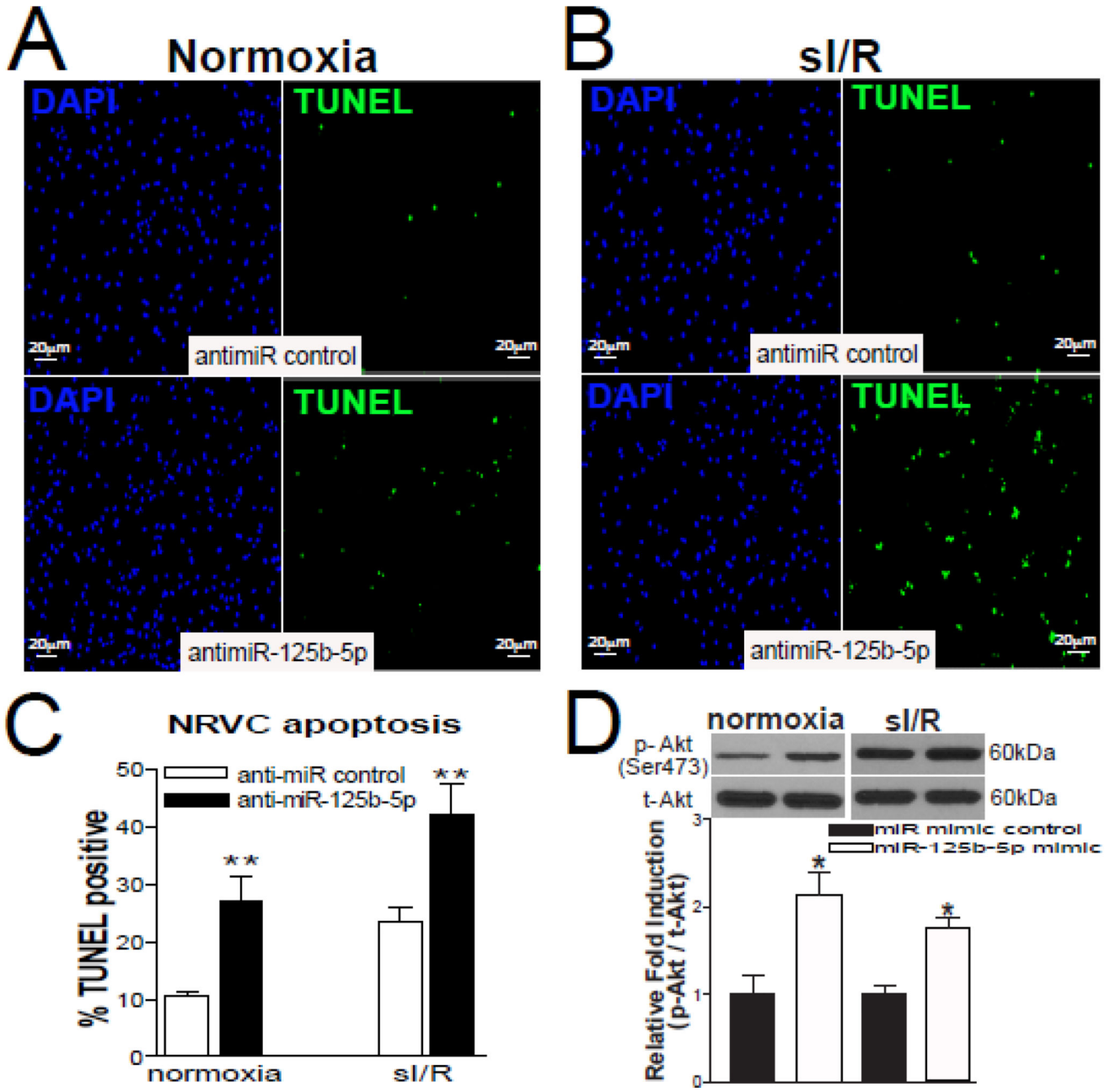

Figure 6. MiR-125b-5p protects against cardiomyocyte apoptosis

A–C, TUNEL analysis of NRVCs transfected with anti-miR control or anti-miR-125b-5p in normoxic (**A and C**) and simulated I/R conditions (**B and C**). The percentage of TUNEL positive cells was normalized to DAPI positive cells (quantified in lower panels). All data are mean ± SEM; N=4. *$P < 0.05$ or **$P < 0.01$ vs. anti-miR control. **D,** Immunoblotting for p-AKT in NRVCs transfected with miR mimic control or miR-125b-5p mimic and subjected to simulated IR. N=4. *$P < 0.05$ vs miR mimic control.

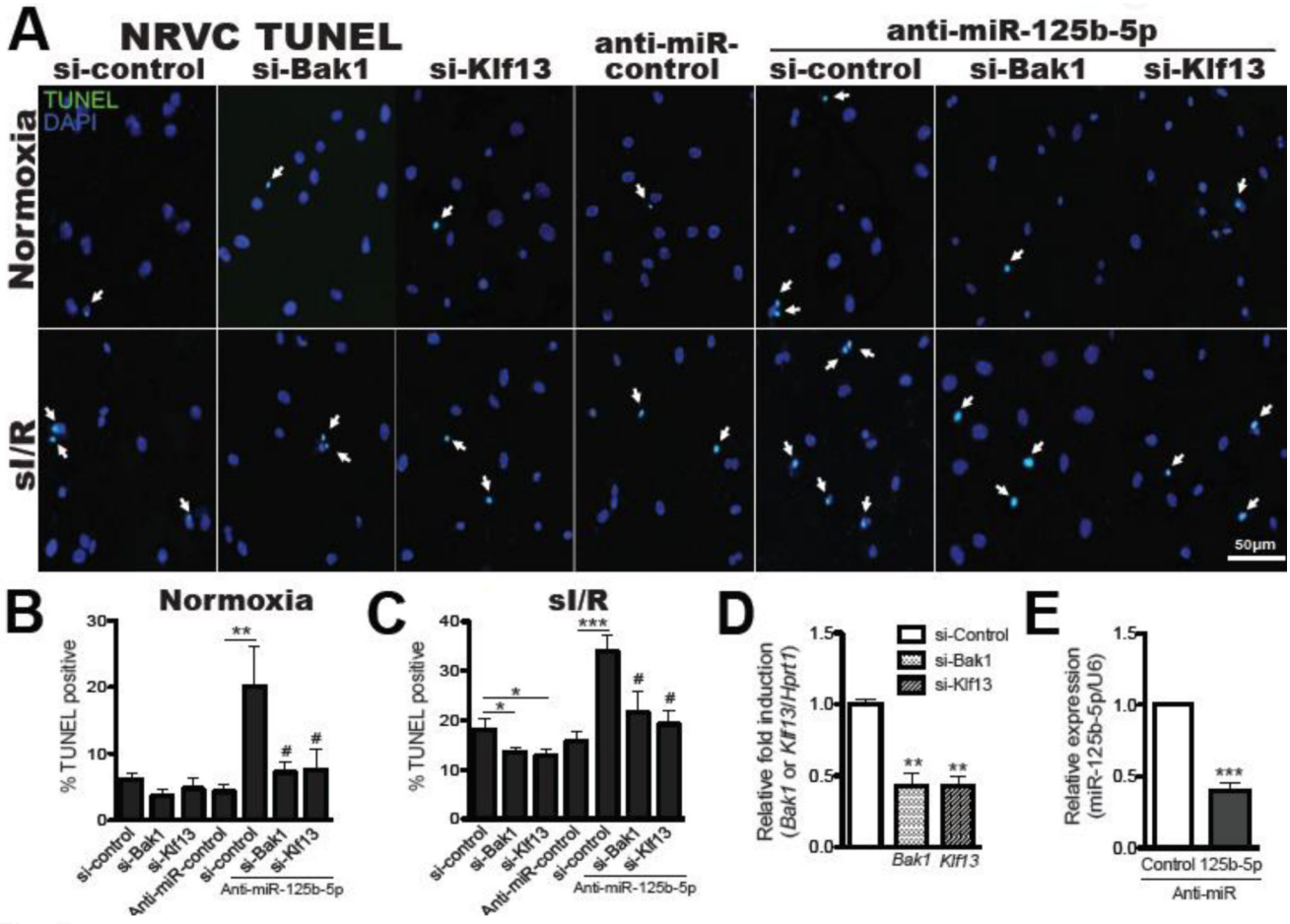

Figure 7. Bak1 and klf13 are necessary for miR-125b-5p-dependent regulation of cardiomyocyte apoptosis

A–E, NRVCs transfected with control scramble siRNA (si-control), bak1 siRNA (si-Bak1), klf13 siRNA (si-Klf13), anti-miR-125b-5p/si-Bak1, or anti-miR-125b-5p/si-Klf13 were subjected to *in vitro* simulation of I/R (sI/R). TUNEL assays were then performed under both basal and sI/R conditions. The percentage of apoptotic nuclei (green) was calculated by normalizing total nuclei (blue). Knockdown of bak1 or klf13 decreases ventricular cardiomyocyte apoptosis and protects NRVCs from the pro-apoptotic effects of anti-miR-125b-5p (**A–C**). QRT-PCR analyses for *bak1* and *klf13* (**D**) and miR-125b-5p (**E**) were performed to verify the knockdown efficiency. Data are shown as mean ± SEM for five independently obtained biological samples. $*P < 0.05$, $**P < 0.01$, or $***P < 0.001$ vs. control : either si-control or anti-miR control. $^{\#}P < 0.05$ vs. anti-miR-125b-5p/si-control.

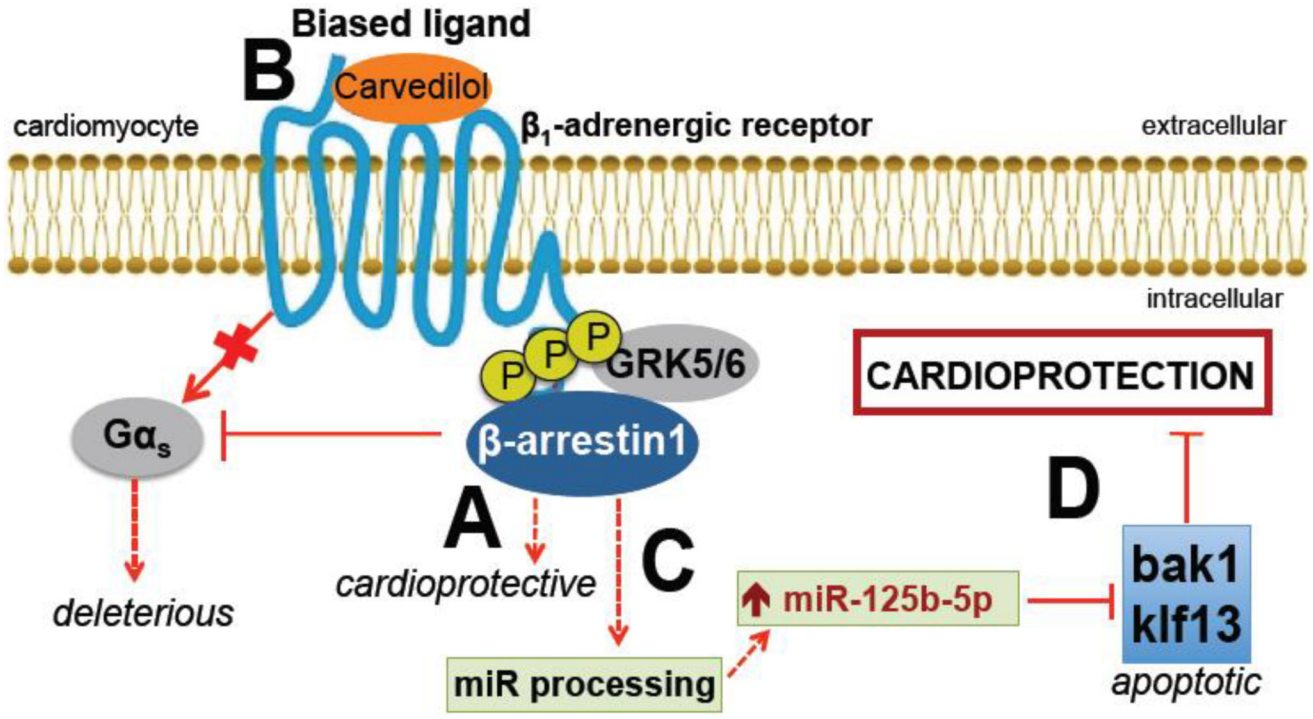

Figure 8. A β_1-adrenergic receptor (β_1AR)/β-arrestin1-responsive miR, miR-125b-5p, is a novel mediator of improved cardiac function and structure after MI

β-arrestin-mediated β_1AR signaling confers cardioprotection [5] (**A**) and the β-blocker carvedilol (Carv) is a β-arrestin-biased ligand for β_1AR [4] (**B**). We previously showed that Carv induces the processing of miR-125b-5p in a β_1AR-, G protein-coupled receptor kinase 5/6 (GRK5/6)- or β-arrestin1-dependent manner [6] (**C**). Here, our results suggest that β-arrestin1-biased agonism of β_1AR-mediated miR-125b-5p processing is a novel cardioprotective mechanism after MI, and that miR-125b-5p confers the improvement of cardiac function and structure after MI by repressing apoptotic genes *bak1* and *klf13* in cardiomyocytes (**D**).